Antibacterial activity of nanoporous gold against *Escherichia coli* and *Staphylococcus epidermidis*

Masataka Hakamada*, Seiji Taniguchi†, Mamoru Mabuchi

Department of Energy Science and Technology, Graduate School of Energy Science, Kyoto University, Yoshidahonmachi, Sakyo, Kyoto 606-8501, Japan

* Corresponding author. E-mail: hakamada.masataka.3x@kyoto-u.ac.jp

† Present address: Sapporo Breweries Ltd., 2 Takasecho, Funahashi, Chiba 273-0014, Japan.

Abstract. Conventional metallic antibacterial materials release metal ions and reactive oxygen species (ROS) for killing bacteria. Herein, we found that nanoporous gold (NPG) exhibits antibacterial activity (AA) at an intermediate relative humidity (RH) of 60% against *Escherichia coli* and *Staphylococcus epidermidis*, in contrast to the inert behavior of bulk gold. The dependence of AA on RH, morphological observations of bacteria on NPG, and transcriptomic analyses of NPG-treated *Escherichia coli* were investigated. These observations collectively suggest that biological processes in cell walls containing peptidoglycan and cell membranes are significantly disrupted by direct contact with NPG. Metal ions and ROS were not detected, and therefore are not responsible for the present antibacterial properties of NPG. The catalytic nature of NPG may be responsible for its AA, probably because of lattice distortion at the surface of nanosized ligaments with high curvature.

Keywords: nanostructure; Au; biological

INTRODUCTION

Several metals and alloys such as silver and copper exhibit antibacterial properties, because they release metal ions[1,2] and reactive oxygen species (ROS)[3] in aqueous environments. Certain metallic nanoparticles that release no harmful diffusive species (e.g., metal ions and ROS) also exhibit antibacterial activity, which is due to their incorporation into the cytoplasm of bacteria, and subsequent deterioration of cytoplasmic proteins such as ribosomes.[4–7]

Nanoporous metals are nanostructured materials with open porous structures containing nanometer-scale pores and ligaments.[8] The first electron microscopy observations of nanoporous metals were reported in 1979–1980 by Forty and Durkin,[9,10] and nanoporous metals have since received much interest from researchers in various fields. Nanoporous gold (NPG) has been intensively investigated, because it is easily fabricated by the dealloying of gold-silver alloys. Lattice distortion occurs at the surface of the nanosized ligaments, because of their large curvature. This results in interesting catalysis behavior of NPG in organic reaction that are not observed in bulk gold[11–15]. NPG reportedly exhibits catalytic activity in the oxidation of carbon monoxide[11–13] and methanol[14], in contrast to bulk gold. NPG also catalytically decomposes methyl orange (MO, an organic azo dye), which bulk gold does not.[15] The decomposition kinetics of MO was not simply proportional to the surface area of NPG, which suggests that active sites

due to lattice distortion is important in the catalysis in NPG. Thus, NPG and its catalytic properties strongly affect the stability of surrounding organic matter.

On the other hand, NPG has been also investigated as a substrate for mammalian cells.[16–18] These studies demonstrated that NPG generally does not cause severe deactivation of cells, although individual processes such as adhesion and growth are sensitive to the porosity of NPG. To our knowledge, however, there have been few reports on the effect of NPG on the activity of bacteria,[19] which have a different composition and structure from those of mammalian cells.

The activity of bacteria is generally sensitive to the surface morphology of nanomaterials.[20] Rizzello et al. reported that the fimbriae of bacteria disappeared on a gold substrate containing nanoscale surface features, while fimbriae were still observed on a flat gold substrate.[21] The effects of nanostructured substrates on the activity of adherent bacteria have been widely investigated, although the underlying mechanism is still in debate.

Bacteria are systematically and functionally assembled organic matters. NPG may therefore catalytically decompose organic materials within the components of bacteria, thus suppressing bacterial activity because NPG strongly affects the stability of surrounding organic matter as described in the

second paragraph. This led us to investigate the antibacterial properties of NPG against *Escherichia coli* (*E. coli*) and *Staphylococcus epidermidis* (*S. epidermidis*). We found that NPG can catalytically damage these bacteria without exploiting diffusive bacteria-killing species such as metal ions and ROS.

EXPERIMENTAL METHODS

A. Preparation of NPG and FG substrates

Gold-silver films sputtered on glass substrates were dealloyed in concentrated nitric acid at 253 and 298 K for 24 h, to fabricate NPG substrates with different ligament sizes. A radio-frequency sputtering apparatus (SVC-700RF, Sanyu Electron Co., Ltd.) was used to fabricate the gold-silver alloy thin film, which was then dealloyed to form NPG. A 50-nm-thick pure gold film (>99.9 mass%) was sputtered on a glass substrate of length × width × thickness of 50 × 50 × 1.2 mm. A 50-nm-thick $Au_{0.47}Ag_{0.53}$ alloy was then sputtered on the gold thin film. NPG was synthesized by dealloying (free corrosion) of the alloy at 253 or 298 K for 24 h, in 69 mass% HNO_3. The microstructures of NPG and FG were observed using SEM (SU-6600; Hitachi High-Technologies Corporation, Tokyo, Japan) equipped with an EDXS apparatus. For comparison, a polyethylene (PE) film and 50-nm-thick flat gold (FG) sputtered on glass were also prepared.

B. Bacterial strain.

Type strains of *E. coli* (K-12, NBRC 3301) and *S. epidermidis* (NBRC 100911) were obtained from the National Institute of Technology and Evaluation (Tokyo, Japan). We incubated bacteria in Luria–Bertani (LB) medium at 308 K for 48 h, before treating in antimicrobial tests. Casein-peptone glucose yeast extract agar (Wako Pure Chemical Industries Ltd., Osaka, Japan) was used for the incubation.

C. Tests of antibacterial activities.

The antibacterial properties of NPG, FG and control PE were tested, essentially according to the Japanese Industrial Standard “Antibacterial products—Test for antibacterial activity and efficacy”.[22] Control PE was necessarily used for the confirmation of validness of each test, although its physical and chemical states of surface differs from those of gold. First, one quantity of platinum loop of bacteria incubated in medium was removed from the colony and placed in 5 mL of 1/500 nutrient broth, followed by vortex mixing. Second, 400 μL of the bacterial suspension was dropped onto the samples and then PE film covered with bacterial suspension. In this way, bacterial suspensions were incubated on samples for a given period (up to 24 h), in humidity-controlled incubators at 308 K. Finally, the incubated bacteria were recovered and diluted in LB medium, to make a 10-fold dilution series of agar pour plates. These

were then incubated at 308 K for 48 h. The number of colonies in the agar pour plates were then counted. The identical tests were repeated 4 times. VBCs were statistically analyzed by one-way analysis of variance followed by a post hoc test. All results were expressed as mean ± standard deviation. Difference were considered statistically significant at p-value < 0.05.

D. Observation of bacteria

The size and morphology of the bacteria incubated for 24 h on the NPG and FG substrates were examined by SEM. Quantitative information on the three-dimensional geometry of *E. coli* was also collected by SPM (NanoWizard III, JPK instruments AG, Berlin, Germany). Prior to SEM and SPM analyses, bacteria on the samples were fixed with 2% glutaraldehyde solution for 2 h, which was then removed by rinsing with phosphate-buffered saline (PBS), after which specimens were dehydrated in a series of ethanol solutions (50, 60, 70, 80, 90, 99, and 100 vol.%) and in *tert*-butyl alcohol. The samples were then freeze-dried from *tert*-butyl alcohol, and coated with Pt-Pd of thickness of 10 nm.

E. Transcriptomic analyses

The expressions of two different genes (*fimA* and *lrhA*) were investigated for *E. coli* cultured in suspension on NPG and FG (24 h, RH of 60%) by real-time polymerase chain reaction (PCR).[21] The

gapA gene, encoding D-glyceraldehyde-3-phosphate dehydrogenase A, was used as an independent internal control. After incubation on substrates (three independent biological replicates), the surfaces were washed out with a mixture of RNAprotect Bacteria Reagent (1000 µL) + PBS (500 µL) (pH 7.5), which stripped the bacteria from the substrates. The total RNA was extracted from the bacterial cells from the NPG and FG samples, using tris-ethylenediaminetetraacetic acid (Tris-EDTA) buffer solution containing lysozyme. The PCR was carried out against the total RNA.

The expression of approximately 5,000 genes was investigated for *E. coli* cultured on NPG and FG (24 h, RH of 60%), by microarray analyses.[5] *E. coli* were collected from four independent biological replicates by centrifugation at 8,000 rpm for 5 min, for the microarray analyses. Samples were hybridized for 16 h on Affymetrix GeneChip *E. coli* Genome 2.0 Array containing approximately 10,000 probe sets for all 20,366 genes. We analyzed the microarray data by Significance Analysis of Microarrays using Genechip Operating Software ver1.4 (Affymetrix). Genes were considered as being regulated with greater than or equal to 2-fold change, meanwhile the *p*-value was required to be below 0.05. We performed DAVID (Database for Annotation, Visualization and Integrated Discovery) analysis[23] for comparison of the expression data. We imported lists of regulated genes to generate the Gene Ontology (GO) enrichment lists.

III. RESULTS

A. Synthesis and characterization of NPG

Scanning electron microscopy (SEM) images of the surface microstructure of the synthesized NPG are shown in FIG. 1. A nanoporous structure with average ligament and pore sizes of approximately 20 nm was observed for the NPG fabricated by dealloying at 253 K. The NPG fabricated by dealloying at 298 K had larger ligament and pore sizes of approximately 50 nm. Energy-dispersive X-ray spectroscopy (EDXS) analysis was carried out during SEM observations. EDXS revealed that the residual Ag content was very small, being below the 1 at.% detection limit (see Supplementary Material for EDXS results). On the other hand, control PE film and FG sputtered on glass did not possess nanoporous structures (see Supplementary Material for SEM image of FG). Water wettability of NPG and FG was similar during our experimental handling, although strict evaluation such as contact angle measurement was not conducted.

B. Antibacterial properties of NPG.

Figure 2 shows viable bacteria counts (VBCs) of *E. coli* and *S. epidermidis* on NPG and FG after incubation for 24 h at various RH. At an intermediate RH of 60%, the VBCs on NPG were much lower

than those on FG. FG showed no significant decrease in the VBCs of *E. coli* and *S. epidermidis* on its surface, compared with the control PE film, which was absent of antibacterial properties. These results indicated that at intermediate RH, NPG possessed antibacterial properties against *E. coli* and *S. epidermidis*, while FG did not. NPG with a pore size of 20 nm reduced the VBCs of both bacteria more efficiently than NPG with a pore size of 50 nm. The VBCs on NPG at a high RH of 90% showed no significant difference to those on FG and the control PE film. The VBCs on NPG at a low RH of 15% were also slightly lower than those on FG and the control PE film. Irrespective of the substrate, a lower RH significantly decreased the VBCs, and a higher RH increased the VBCs. This was attributed to drying and is explained later. These results suggested that the antibacterial properties of NPG were significant at intermediate RH, which may have practical importance.[24–26]

The antibacterial activity (*AA*) of nanoporous Au can be expressed by:

$$AA = \log_{10}(N_0/N), \quad (1)$$

where N_0 and N are the VBCs on FG (as a control sample) and NPG, respectively. When the *AA* is >2.0, *i.e.* when the reduction in VBC by the sample is >99%, then the material is generally regarded as antibacterial.[22] The relationships between the *AA* of NPG and RH with respect to *E. coli* and *S. epidermidis* are shown in FIG. 3a and b, respectively. NPG exhibited the best antibacterial performance

at an intermediate RH of 60%. The antibacterial properties diminished at lower or higher RH. NPG with a pore size of 20 nm exhibited better antibacterial performance than that with a pore size of 50 nm. This suggested that the small pores and ligaments were the source of the antibacterial properties in NPG. Figure 3b shows that the *AA* of NPG against *S. epidermidis* was approximately 0.7 at low RH, while that of NPG against *E. coli* was approximately zero. The slightly higher AA of NPG against *S. epidermidis* was due to the fact that gram-positive *S. epidermidis* is more resistant towards dryness than *E. coli* because of thicker cell wall, and that the N_0 of *S. epidermidis* was somewhat higher than the *N* (see FIG. 2b). Thus, *S. epidermidis* can live to some extent at low RH. However, NPG still affected the VBC of *S. epidermidis* at the low RH.

Subsequent investigations were carried out using the NPG with the pore size of 20 nm, because of its higher *AA*. Figure S3 in Supplementary Material shows the variation in VBCs of *E. coli* on NPG and FG with incubation time, at a RH of 60%. The VBC on NPG was lower than that on FG at every incubation time. The VBCs on NPG incubated for 12–24 h were significantly lower than those on FG, at the corresponding incubation times. The VBCs on NPG and FG were similar for incubation times of 0–12 h. Thus, antibacterial properties of NPG were evident after incubation for 12 h at a RH of 60%. This behavior is quite different from the antibacterial activity by metal ions, which typically begin decreasing

the VBC immediately after commencing incubation.[1]

C. Morphological observations of treated bacteria.

SEM images of *E. coli* on NPG (pore size of 20 nm) and FG are shown in FIG. 4. The shape of *E. coli* on NPG was significantly distorted, with a dimple observed in the center of the cell (FIG. 4a). Leakage of the cytoplasm was also apparent, as shown by arrows in FIG. 4b. The cell membrane of *E. coli* cultured on FG was not distorted (FIG. 4c), as an undented rod shape was observed. No fimbria were observed in the SEM images of *E. coli* on both NPG and FG,[21] perhaps because of the intermediate RH.

Similar trends were observed for *S. epidermidis*, as shown in FIG. 5. The membrane of *S. epidermidis* on NPG was damaged, and its morphology was aspherical. Isolated bacteria were also frequently observed. The cell wall of *S. epidermidis* cultured on FG was not damaged, and several bacteria formed grape-shaped clusters, which is typical of active *Staphylococcus* bacteria.

Scanning probe microscope (SPM) were used to quantify the shape distortion of *E. coli* on NPG, as shown in FIG. 6. Figure 6a shows the morphology of *E. coli* on NPG, as observed by SPM. The bacteria appeared dented, similarly to in the SEM observations. The height profile of the *E. coli* cell collected along its long axis (FIG. 6b) showed an obvious concave structure at the cell center. The dimple depth

and maximum height of the *E. coli* cell are collected from the SPM observations of *E. coli* on NPG. The dimple depth is the height difference between highest point and lowest point of the dimple (FIG. 6b). The maximum height of the *E. coli* cell is the height difference between the highest point and the base of the *E. coli* cell (FIG. 6b). Average values of dimple depth and maximum height, as determined from measurements of more than 20 individual *E. coli* cells, are summarized in FIG. 6d. The average dimple depth of *E. coli* on NPG was 55 nm, which was much larger than that of *E. coli* on FG (9 nm). The average maximum height of *E. coli* on NPG was 109 nm, which was smaller than that of *E. coli* on FG (198 nm). These data indicated that the *E. coli* cell was severely flattened and dimpled on NPG. The SPM measurements indicated the detrimental effect of the NPG structure on the shape of *E. coli* cells. This correlated with the antibacterial activity of NPG.

D. Transcriptomic analysis

The gene expression related to the fimbriae evolution of *E. coli* was differentiated in a previous study.[21] To compare the gene expression of *E. coli* on the present gold samples with that reported previously, the expression levels of two genes related to fimbria evolution were analyzed by real-time polymerase chain reaction (PCR). The results are summarized in FIG. 7. Two genes of *fimA*, which encodes the major subunit of type-1 fimbriae, and *lrhA*, which encodes the repressor of the *fim* operon, were investigated.

The mRNA expression level for *fimA* in *E. coli* grown on NPG was clearly higher than that in *E. coli* grown on FG. In contrast, *lrhA* in *E. coli* grown on NPG was expressed at a slightly lower level than that of *E. coli* grown on FG. The *p*-values of expression levels of *fimA* and *lrhA* were 0.000087 and 0.54, respectively. Thus, there was a clear difference in the expression level of *fimA* between NPG and FG, but not for *lrhA*.

To comprehensively investigate the effects of the antibacterial NPG on *E. coli*, mRNA expression was analyzed by gene microarray hybridization. Across the GO databases, differently expressed genes in several classifications including physiological process, cellular processes, catalytic activity, metabolism, binding, transporter activity, protein complex and localization, were identified. According to filtering criteria, 99 genes were differentially expressed in *E. coli* cultured in the medium on NPG, among which 24 were up-regulated and 75 were down-regulated. Based on the biological process, molecular function, and cellular component classification, these up- or down-regulated genes were classified to different GO terms. We investigated three classifications related to up-regulated and down-regulated genes by GO enrichment analysis, as summarized in Tables I and II. Stricter filtering criteria with fold changes of >3 and p-values of <0.01 detected the significant down-regulation of *c0412*, *cpxP*, *ytfQ* and *htpX*, which are related to the membrane system in the cell envelope of *E. coli*.[27–34]

IV. DISCUSSION

We observed that the thickness of bacterial suspension on samples reduced because of evaporation at RH values of 15% and 60%. The suspension volume was largely unchanged after incubation for 24 h at RH of 90%. This suggested that the effect of RH on the antibacterial properties of NPG was related to the thickness of the suspension, as illustrated in FIG. 8. A low RH of 15% caused significant drying and subsequent bacterial death on NPG and FG. In this case, the *AA* of NPG was not overly high, because N_0 and N in equation (1) were similar. A high RH of 90% minimized evaporation of the suspension during incubation. Bacteria in the suspension could live and proliferate far from substrate surface without contacting the NPG substrate, resulting in low *AA*. The intermediate RH of 60% apparently resulted in reduced residual bacterial solution to force the bacteria to contact with the NPG substrate. Hence, the direct contact of bacteria with the NPG substrate was necessary for the antibacterial efficacy of NPG.

The time variation in the VBC cultured in suspension on NPG (FIG. S3) also supported the necessity of direct contact between the bacteria and NPG. The suspension thickness gradually decreased during incubation for 24 h at a RH of 60%. The VBC on NPG significantly decreased only after 12 h of incubation, where the dryness of samples caused the decrease in suspension volume and bacteria are forced to touch NPG substrates. These results strongly implies that antibacterial properties of NPG are

attributed to the catalytic nature of NPG, and not to the metallic ion and reactive oxygen species (ROS) released into the solution from substrates (if these diffusible species were responsible for the antibacterial properties of NPG, *AA* at RH = 90% would be higher due to the diffusion of these species.) We also confirmed that metal ions (silver and gold) and ROS were essentially absent in the culturing solution, as described in Supplementary Material. Thus, NPG itself directly and catalytically deteriorated the bacteria. The range of the catalytic effect of NPG was thought to be limited to within a few nanometers from the surface.[35] Hence, direct contact between the bacteria and NPG was necessary for antibacterial activity. The *AA* of NPG with a smaller pore size was stronger than that of NPG with a larger pore size. A smaller ligament size provided a higher concentration of catalytically active sites on the ligament surface. This resulted from the more pronounced lattice distortion and higher concentration of atomic defects at the higher curvature ligaments.

The *AA* of NPG depended on direct contact of the bacteria with the NPG surface. SEM and SPM observations indicated severe distortion in the bacterial shape on NPG. Thus, the nanosized ligaments of NPG directly influenced the physical and/or chemical stability of the bacterial cell wall and membrane, resulting in their death.

In a previous study, the fimbriae of *E. coli* on nanorough gold synthesized by electroless deposition

disappeared, while the fimbriae of *E. coli* on FG could be observed.[21] Real-time PCR analyses indicated that the mRNA expression level for *fimA* in *E. coli* cultured on nanorough gold was lower than that in *E. coli* cultured on FG, and that the mRNA expression level for *lrhA* in *E. coli* cultured on nanorough gold was higher than that in *E. coli* cultured on FG. This indicated that nanorough gold resulted in the fimbriae of *E. coli* disappearing, from a transcriptomic point of view. In the present study, the mRNA expression level for *fimA* in *E. coli* cultured on NPG was higher than that in *E. coli* cultured on FG. In other words, the real-time PCR result in the present study was opposite to that in the previous study. This difference suggested that small changes in the characteristics of nanostructure and lattice strain caused significant transcriptomic differentiation.

Microarray analyses of *E. coli* on NPG showed the significant down-regulation of *c0412*, *cpxP*, *ytfQ*, and *htpX*. The *c0412* gene encodes the transcriptional regulator protein *YcjZ* controlling the recycling of peptidoglycan, which structurally supports the body of *E. coli* in its cell envelope.[36] The *CpxP* protein governs the Cpx pathway of periplasmic stress response, operating as a proteolytic adapter to facilitate degradation of misfolded proteins in the cell envelope.[28] The *YtfQ* protein promotes and supports the importing of nutritious substances in the periplasm.[31] The *htpX* protein induces endoproteolytic cleavage, to facilitate dislocating misfolded membrane proteins out of the membrane.[32–34] Down-regulation of these

genes suggested that NPG directly (not depending on diffusive species such as metal ions and ROS) and catalytically induced the collapse of the cell envelope system of *E. coli*. This inhibited the normal exchange of intracellular and extracellular substances through the cell membrane, inducing protein misfolding and subsequent cell death.

The catalytic degradation of nutritious components in the culturing media by NPG was not responsible for the present antibacterial properties. If it were, then NPG would exhibit antibacterial properties even at a RH of 90%, where nutritious components could degrade at the catalytic NPG substrate. Hence, the direct contact of NPG with the bacterial cell envelope was necessary for killing bacteria, perhaps inducing the catalytic decomposition of envelope-structuring components such as peptidoglycan and membrane proteins. The physical situation may be similar to that nanostructured artificial viruses with antibacterial activity, which bypass the need for membrane-induced folding and destroy bacterial membrane on direct contact.[37] However, it is not currently clear what part of the envelope was catalytically degraded by NPG. This is because even detailed chemical analyses of products from *AA* tests cannot determine the substance directly affected by NPG. The conformation and subsequent stability of proteins in the cell membrane may be altered by NPG,[38,39] as is observed for other porous materials.[40] Several approaches including investigating purified components such as peptidoglycan and synthesized cell membrane proteins are

required for a critical elucidation.

V. CONCLUSIONS

NPG affected biological processes operating in the membrane system of bacteria, resulting in bacterial death under intermediate RH. The antibacterial properties of NPG differed from those of typical antibacterial metals and alloys, because metal ions and ROS were not responsible for bacterial death. The monolithic nanostructure of NPG also differentiated its antibacterial properties from those of metallic nanoparticles, the latter of which typically penetrate the cell envelope, enter, and disturb the cytoplasm of the bacteria. Transcriptomic analyses suggested that NPG degraded the cell envelope of *E. coli*, which correlated with the distorted bacterial shape observed by microscopy. These phenomena may be related to the catalytic properties of NPG, although more evidences will be necessary for further elucidation.

ACKNOWLEDGMENT

M.H. acknowledges financial support by JSPS KAKENHI Grant Number JP15H05547.

Supplementary Material

The Supplementary Material is available free of charge on the Cambridge University Press website at

DOI: (to be inserted).

EDXS results of NPG, SEM of FG, time variation of VBCs on NPG and FG for *E. coli* and metallic ion/ROS concentration in the culturing medium of *E. coli* on NPG.

References

1. G. Zhao, and S. E. Stevens Jr.: Multiple parameters for the comprehensive evaluation of the susceptibility of Escherichia coli to the silver ion. *Biometals* **11**, 27 (1998).

2. B. Galeano, E. Korff, and W. L. Nicholson: Inactivation of vegetative cells, but not spores, of *Bacillus anthracis*, *B. cereus*, and *B. subtilis* on stainless steel surfaces coated with an antimicrobial silver- and zinc-containing zeolite formulation. *Appl. Environ. Microbiol*. **69**, 4329 (2003).

3. A. K. Chatterjee, R. Chakraborty, and T. Basu: Mechanism of antibacterial activity of copper nanoparticles. *Nanotechnology* **25**, 135101 (2014).

4. S. Sadhasivam, P. Shanmugam, M. Veerapandian, R. Subbiah, and K. Yun: Biogenic synthesis of multidimensional gold nanoparticles assisted by *Streptomyces hygroscopicus* and its electrochemical and antibacterial properties. *Biometals* **25**, 351 (2012).

5. Y. Cui, Y. Zhao, Y. Tian, W. Zhang, X. Lü, and X. Jiang: The molecular mechanism of action of bactericidal gold nanoparticles on *Escherichia coli*. *Biomaterials* **33**, 2327 (2012).

6. Y. Zhang, H. Peng, W. Huang, Y. Zhou, and D. Yan: Facile preparation and characterization of highly

antimicrobial colloid Ag or Au nanoparticles. *J. Colloid Interface Sci.* **325**, 371 (2008).

7. J. F. Hernández-Sierra, F. Ruiz, D. C. C. Pena, F. Martínez-Gutiérrez, A. E. Martínez, A. de J. P. Guillén, H. Tapia-Pérez, and G. M. Castañón: The antimicrobial sensitivity of *Streptococcus mutans* to nanoparticles of silver, zinc oxide, and gold. *Nanomed.-Nanotechnol. Biol. Med.* **4**, 237 (2008).

8. J. Erlebacher, M. J. Aziz, A. Karma, N. Dimitrov, and K. Sieradzki: Evolution of nanoporosity in dealloying. *Nature* **410**, 450 (2001).

9. A. J. Forty: Corrosion micromorphology of noble metal alloys and depletion gilding. *Nature* **282**, 597 (1979).

10. A. J. Forty, and P. Durkin: A micromorphological study of the dissolution of silver-gold alloys in nitric acid. *Philos. Mag. A* **42**, 295 (1980).

11. S. Kameoka, and A. P. Tsai: CO oxidation over a fine porous gold catalyst fabricated by selective leaching from an ordered $AuCu_3$ intermetallic compound. *Catal. Lett.* 121, 337 (2008).

12. V. Zielasek, B. Jürgens, C. Schulz, J. Biener, M. M. Biener, A. V. Hamza, and M. Bäumer: Gold catalysts: nanoporous gold foams. *Angew. Chem. Int. Ed.* **45**, 8241 (2006).

13. C. Xu, J. Su, X. Xu, P. Liu, H. Zhao, F. Tian, and Y. Ding: Low temperature CO oxidation over unsupported nanoporous gold. *J. Am. Chem. Soc.* **129**, 42 (2007).

14. A. Wittstock, V. Zielasek, J. Biener, C. M. Friend, and M. Bäumer: Nanoporous gold catalysts for selective gas-phase oxidative coupling of methanol at low temperature. Science **327**, 319 (2010).

15. M. Hakamada, F. Hirashima, and M. Mabuchi: Catalytic decoloration of methyl orange solution by nanoporous metals. *Catal. Sci. Technol.* **2**, 1814 (2012).

16. E. Seker, Y. Berdichevsky, K. J. Staley, and M. L. Yarmush: Microfabrication-compatible nanoporous gold foams as biomaterials for drug delivery. *Adv. Healthc. Mater.* **1**, 172 (2012).

17. Y. H. Tan, S. E. Terrill, G. S. Paranjape, K. J. Stine, and M. R. Nichols: The influence of gold surface texture on microglia morphology and activation. *Biomater. Sci.* 2, 110 (2014).

18. C. A. R. Chapman, H. Chen, M. Stamou, J. Biener, M. M. Biener, P. J. Lein, and E. Seker: Nanoporous gold as a neural interface coating: effects of topography, surface chemistry, and feature size. *ACS Appl. Mater. Interfaces* **7**, 7093 (2015).

19. Santos, G. M., de Santi Ferrara, F. I., Zhao, F., Rodrigues, D. F., and Shih, W.-C.: Photothermal

inactivation of heat-resistant bacteria on nanoporous gold disk arrays. *Opt. Mater. Express* **6**, 1217 (2016).

20. K. Anselme, P. Davidson, A. M. Popa, M. Giazzon, M. Liley, and L. Ploux: The interaction of cells and bacteria with surfaces structured at the nanometre scale. *Acta Biomater.* **6**, 3824 (2010).

21. L. Rizzello, B. Sorce, S. Sabella, G. Vecchio, A. Galeone, V. Brunetti, R. Cingolani, and P. P. Pompa, Impact of nanoscale topography on genomics and proteomics of adherent bacteria. *ACS Nano* 5, 1865 (2011).

22. Japanese Standards Association, Japanese Industrial Standard (JIS) Z 2801 Antibacterial products—Test for antibacterial activity and efficacy.

23. DAVID Bioinformatics Resources 6.7, http://david.abcc.ncifcrf.gov/ (accessed 27 December 2016)

24. T. Møretrø, and S. Langsrud: Effects of materials containing antimicrobial compounds on food hygiene. *J. Food Prot.* **74**, 1200 (2011).

25. Y. Hirai: Survival of bacteria under dry conditions; from a viewpoint of nosocomial infection. *J. Hosp. Infect.* **19**, 191 (1991).

26. T. Møretrø, G. S. Høiby-Pettersen, C. K. Halvorsen, and S. Langsrud: Antibacterial activity of cutting boards containing silver. *Food Control* **28**, 118 (2012).

27. P. N. Danese, and T. J. Silhavy: CpxP, a stress-combative member of the Cpx regulon. *J. Bacteriol.* 180, 831 (1998).

28. G. L. Thede, D. C. Arthur, R. A. Edwards, D. R. Buelow, J. L. Wong, T. L. Raivio, and J. N. M. Glover: Structure of the periplasmic stress response protein CpxP. *J. Bacteriol.* **193**, 2149 (2011).

29. M. Miot, and M. Betton: Optimization of the inefficient translation initiation region of the *cpxP* gene from *Escherichia coli*. *J. Protein Sci.* **16**, 2445 (2007).

30. B. P. Lima, H. Antelmann, K. Gronau, B. K. Chi, D. Becher, S. R. Brinsmade, and A. J. Wolfe: Involvement of protein acetylation in glucose-induced transcription of a stress-responsive promoter. *Mol. Microbiol.* **81**, 1190 (2011).

31. R. S. P. Horler, A. Müller, D. C. Williamson, J. R. Potts, K. S. Wilson, and G. H. Thomas: Furanose-specific sugar transport characterization of a bacterial galactofuranose-binding protein. *J. Biol. Chem.* **284**, 31156 (2009).

32. Y. Akiyama: Quality control of cytoplasmic membrane proteins in *Escherichia coli*. *J. Biochem.* **146**, 449 (2009).

33. P. P. Coltri, and Y. B. Rosato: Regulation of the htpX gene of *Xylella fastidiosa* and its expression in *E. coli*. *Curr. Microbiol.* **48**, 391 (2004).

34. N. Shimohata, S. Chiba, N. Saikawa, K. Ito, and Y. Akiyama: The Cpx stress response system of *Escherichia coli* senses plasma membrane proteins and controls HtpX, a membrane protease with a cytosolic active site. *Genes Cells* **7**, 653 (2002).

35. A. E. Nel, L. Mädler, D. Velegol, T. Xia, E. M. V. Hoek, P. Somasundaran, F. Klaessig, V. Castranova, and M. Thompson: Understanding biophysicochemical interactions at the nano–bio interface. *Nat. Mater*. **8**, 543 (2009).

36. T. Shimada, K. Yamazaki, and A. Ishihama: Novel regulator PgrR for switch control of peptidoglycan recycling in *Escherichia coli*. *Genes Cells* **18**, 123 (2013).

37. Castelletto V., de Santis, E., Alkassem, H., Lamarre, B., Noble, J. E., Ray, S., Bella, A., Burns, J. R., Hoogenboomb, B. W., and Ryadnov, M. G.: Structurally plastic peptide capsules for synthetic

antimicrobial viruses. *Chem. Sci.* **7**, 1701 (2016).

38. M. Hakamada, M. Takahashi, and M. Mabuchi: Enhanced thermal stability of laccase immobilized on monolayer-modified nanoporous Au. *Mater. Lett.* **66**, 4 (2011).

39. O. V. Shulga, K. Jefferson, A. R. Khan, V. T. D'Souza, J. Liu, A. V. Demchenko, and K. J. Stine: Preparation and characterization of porous gold and its application as a platform for immobilization of acetylcholine esterase. *Chem. Mater.* 19, 3902 (2007).

40. S. Hudson, J. Cooney, and E. Magner: Proteins in mesoporous silicates. *Angew. Chem. Int. Ed.* **47**, 8582 (2008).

Figure captions

FIG. 1. SEM images of NPG. Samples were fabricated by dealloying at (a) 253 K and (b) 298 K, in 69 mass% HNO_3. The lower dealloying temperature led to smaller pore and ligament sizes.

FIG. 2. Viable bacterial counts (VBCs) on NPG, FG, and control PE films as a function of relative humidity (RH), for 24 h incubation of (a) *E. coli* and (b) *S. epidermidis*. * denotes significant difference between NPG and FG with $p < 0.05$, while # denotes significant difference between NPG (20 nm) and NPG (50 nm) with $p < 0.05$. An intermediate RH of 60% differentiated the VBCs on NPG from those on FG, while lower and higher RHs did not. (color online)

FIG. 3. Antibacterial activities (AAs) of NPG as a function of RH, for 24 h incubation of (a) *E. coli* and (b) *S. epidermidis*. The maximum AA against both bacteria was observed at the intermediate RH. (color online)

FIG. 4. SEM images of *E. coli* cultured on NPG and FG at RH = 60%. (a) The center of the cell of *E. coli* on NPG appeared dimpled. (b) Cytoplasm leaked from *E. coli* on NPG (arrows). (c, d) No dimpling and cytoplasm leakage were observed in *E. coli* on FG.

FIG. 5. SEM images of *S. epidermidis* cultured on NPG and FG at RH = 60%. (a) The cell wall of *S. epidermidis* on NPG was significantly distorted. (b) Isolated *S. epidermidis* cells were frequently observed on NPG. (c) The cell wall of *S. epidermidis* on FG was not damaged, and bacteria tended to form grape-shaped clusters, which is typical of active *Staphylococcus* bacteria.

FIG. 6. SPM images of *E. coli* cultured on NPG at RH = 60%. (a) The center of the cell of *E. coli* on NPG was dimpled. (b) Height profile of the *E. coli* cell along the dashed line in (a). (c) Dimple depth and maximum height for *E. coli* cells on NPG and FG. The dimple was deeper in the *E. coli* cell on NPG, than on FG. The maximum height was greater in the *E. coli* cell on FG, than on NPG. The shape distortion was more severe in the *E. coli* cell on NPG, than on FG. (color online)

FIG. 7. Expression levels of *lrhA* and *fimA* in *E. coli* on NPG compared with *E. coli* on FG. RH during culturing was 60%. *fimA* was expressed more in *E. coli* on NPG. *lrhA* in *E. coli* on NPG was expressed at a similar level to that in *E. coli* on FG.

FIG. 8. Schematic illustration of humidity dependence of antibacterial activity (AA) of NPG. The evaporation of bacterial suspension was related to the high AA at intermediate relative humidity (RH). This suggested that the direct contact of bacteria with the catalytic NPG substrate was necessary for AA.

Tables

Table I. Significantly down-regulated biological processes in *E. coli* on NPG.

GO term	Gene number
Ribosome	5
Membrane or periplasm	19
Metabolic process	12
DNA binding	10
Ion binding	6

Table II. Significantly up-regulated biological processes in *E. coli* on NPG.

GO term	Gene number
Ribosome	6
Metal ion binding or transport	5
Periplasm	3

FIG. 1

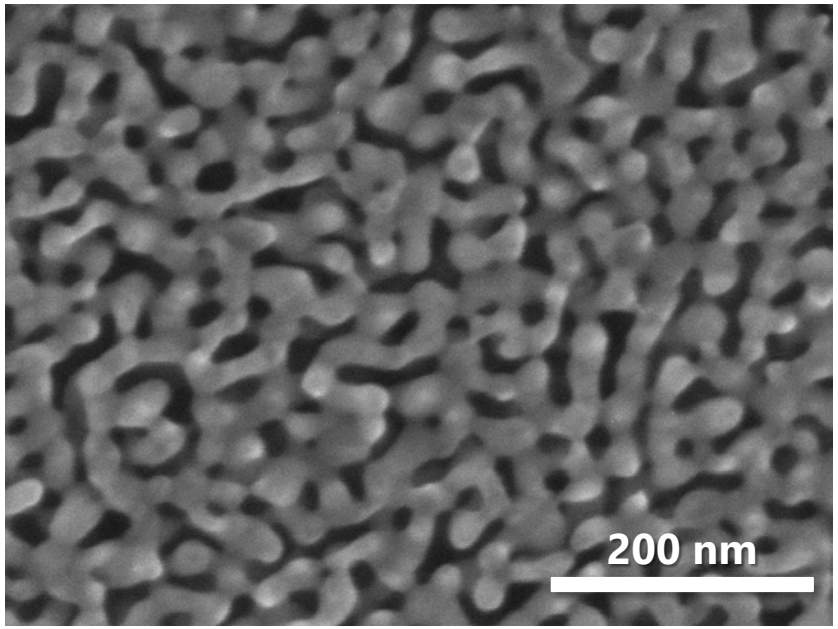

(a)

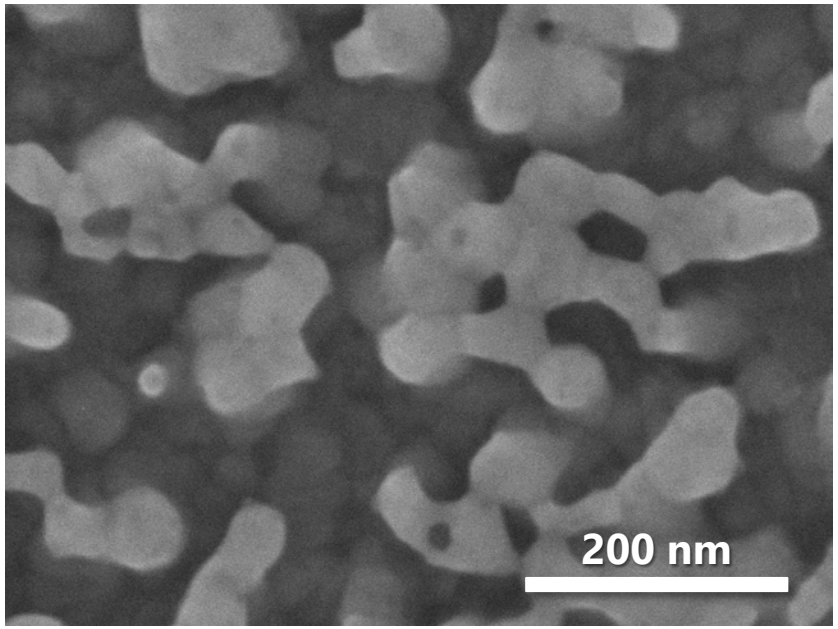

(b)

FIG. 2

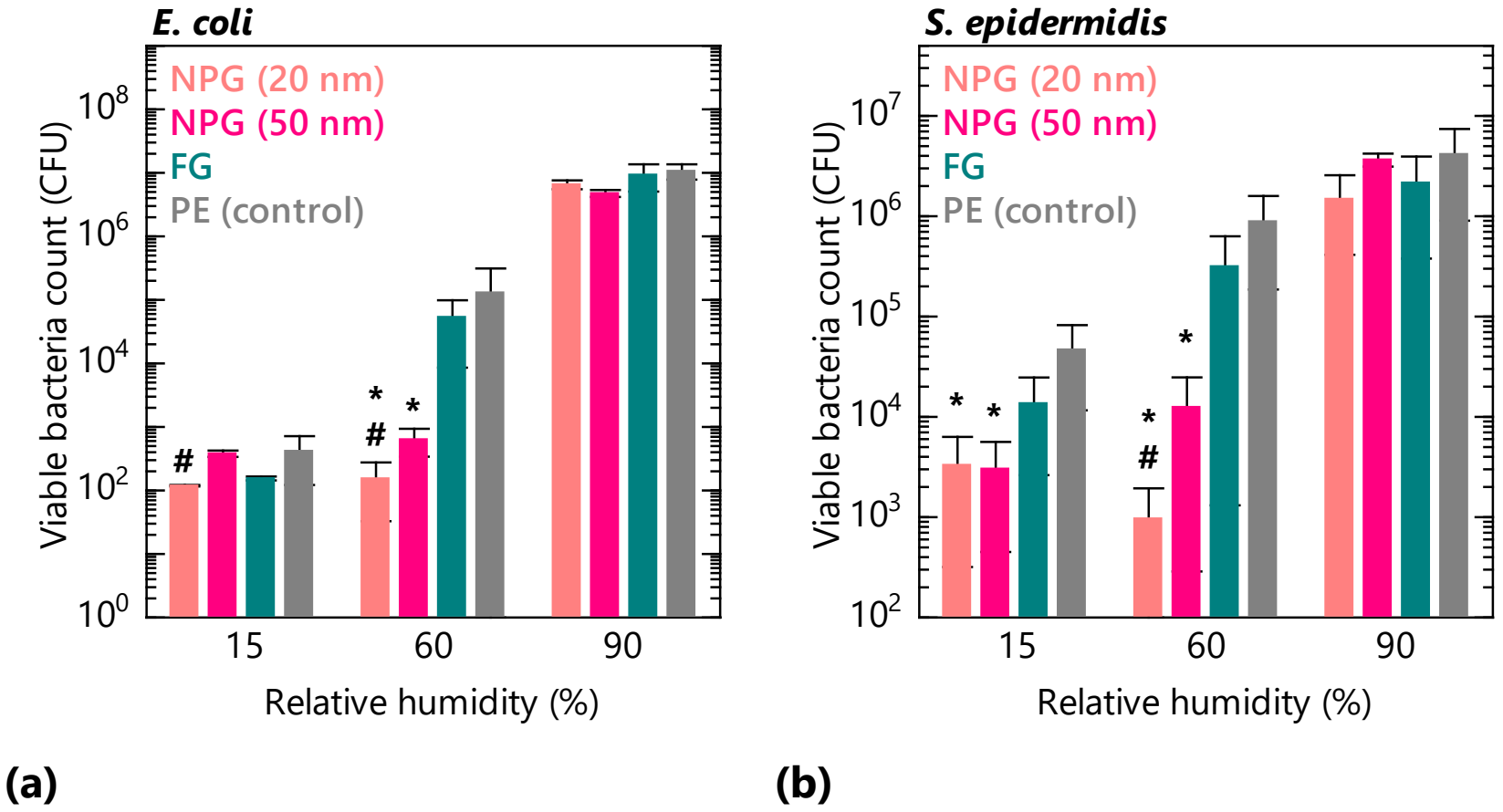
E. coli
NPG (20 nm)
NPG (50 nm)
FG
PE (control)
Viable bacteria count (CFU)
10^0
10^2
10^4
10^6
10^8
15
60
90
Relative humidity (%)
#
*
*
#
*
*
(a)
S. epidermidis
NPG (20 nm)
NPG (50 nm)
FG
PE (control)
Viable bacteria count (CFU)
10^2
10^3
10^4
10^5
10^6
10^7
15
60
90
Relative humidity (%)
*
*
*
#
*
(b)

FIG. 3

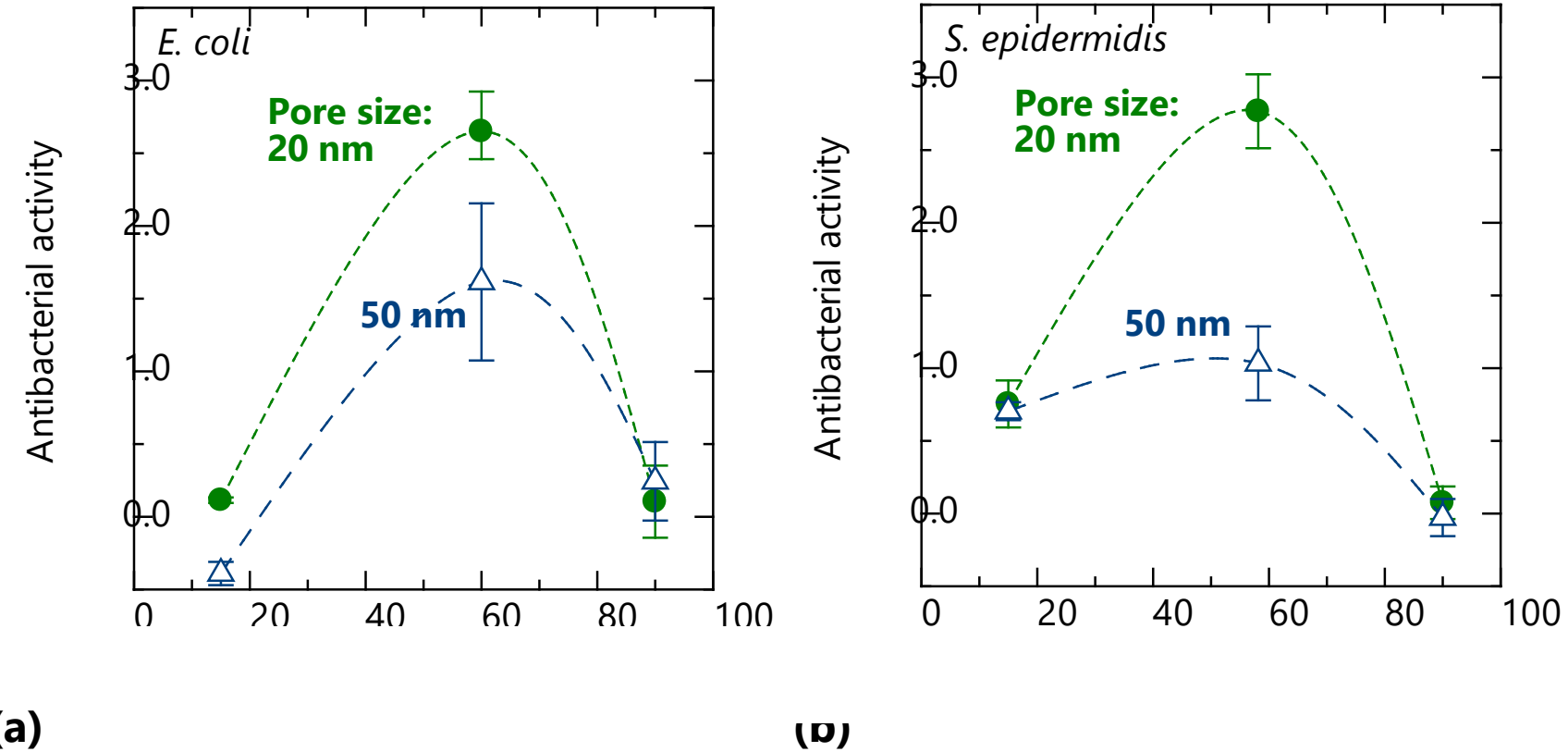
E. coli
Pore size:
20 nm
50 nm
Antibacterial activity
0.0
1.0
2.0
3.0
0
20
40
60
80
100
(a)
S. epidermidis
Pore size:
20 nm
50 nm
Antibacterial activity
0.0
1.0
2.0
3.0
0
20
40
60
80
100
(b)

FIG. 4

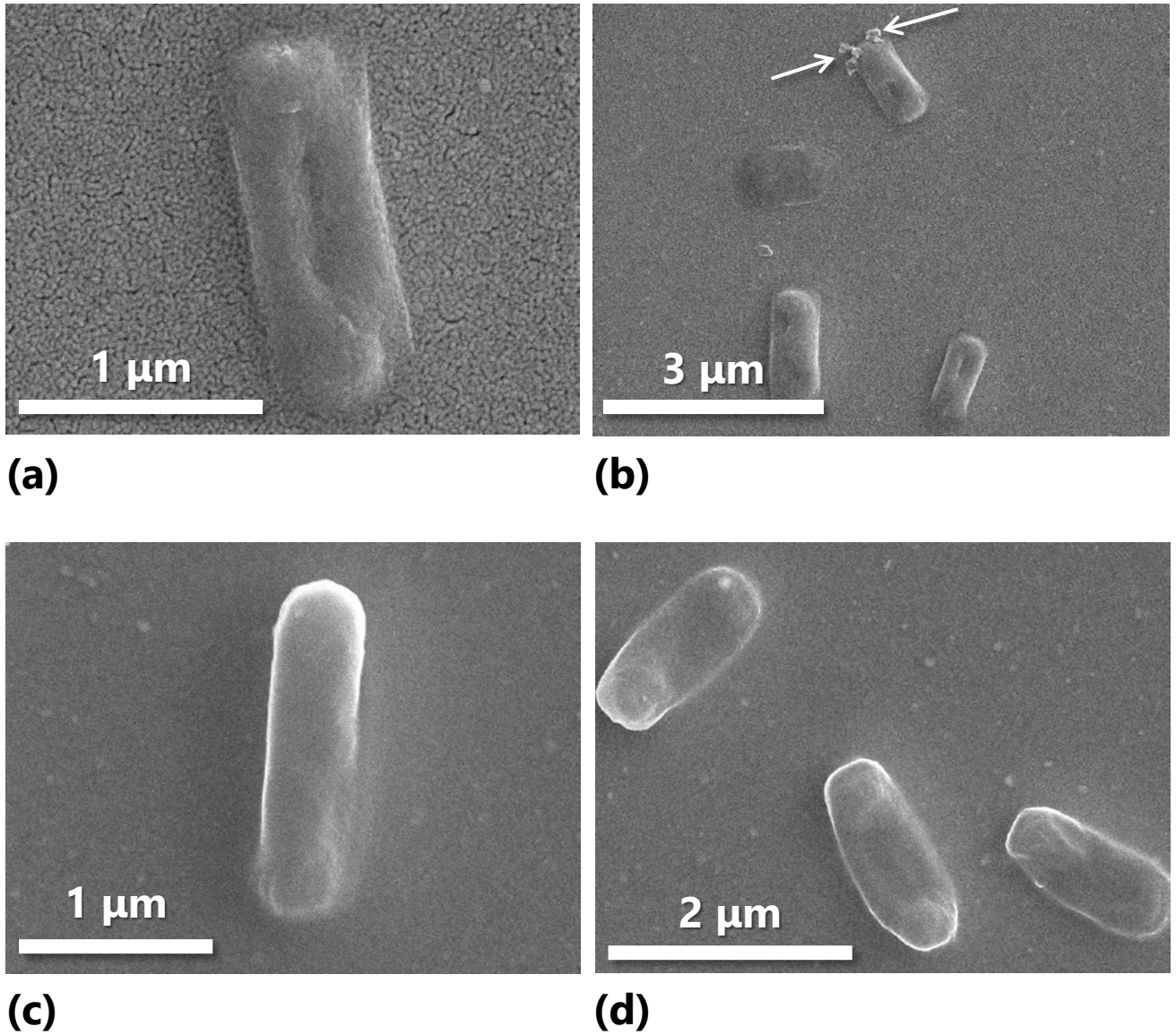

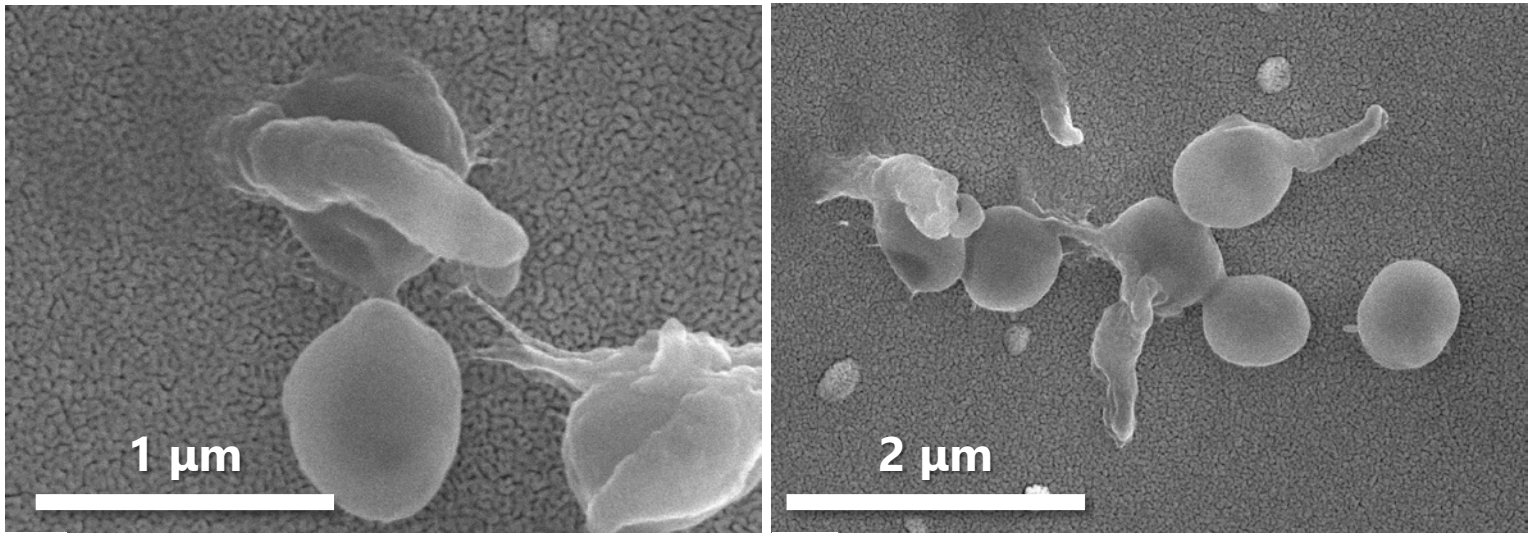

(a) (b)

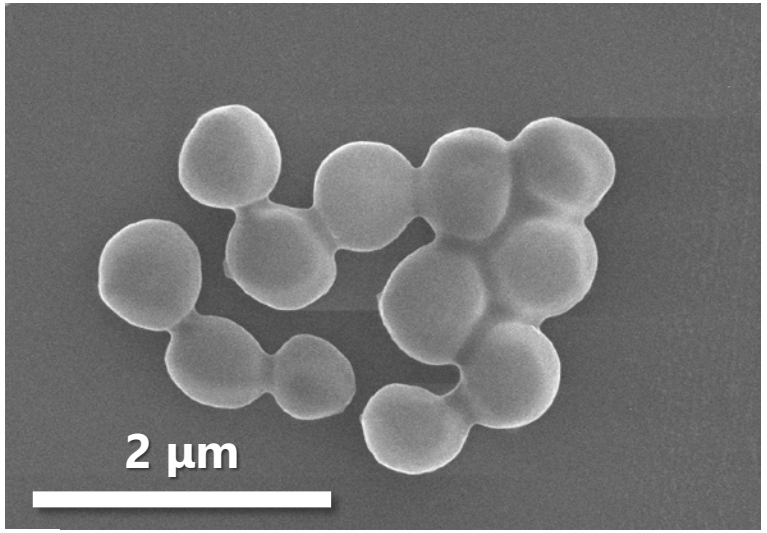

(c)

FIG. 5

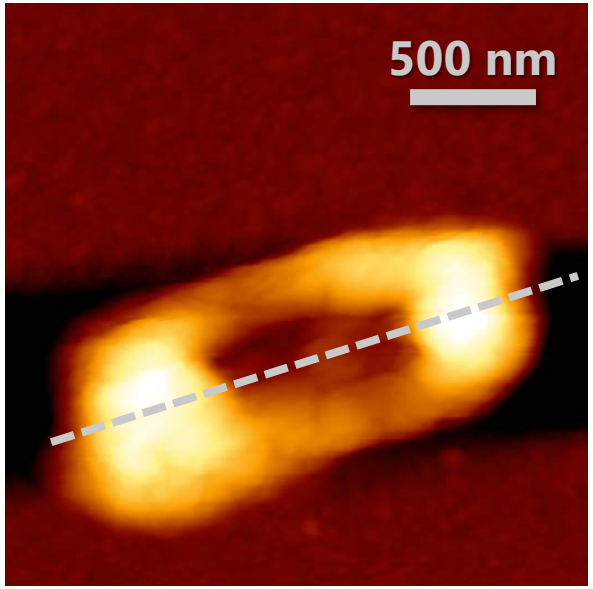
500 nm

(a)

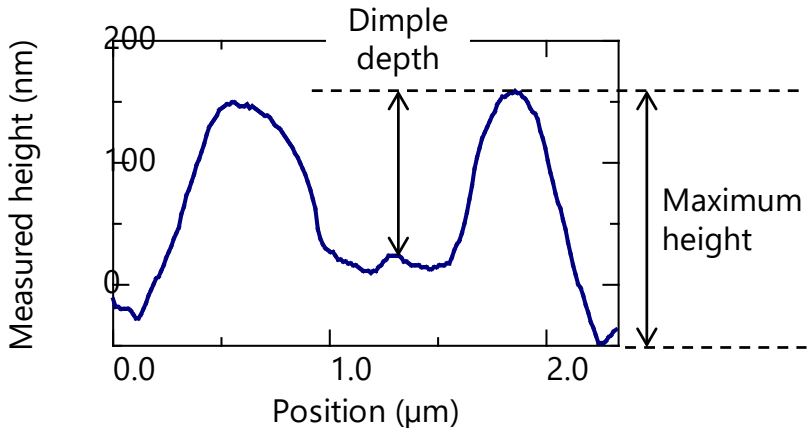
Dimple depth
Maximum height
Measured height (nm)
200
100
0
0.0
1.0
2.0
Position (μm)

(b)

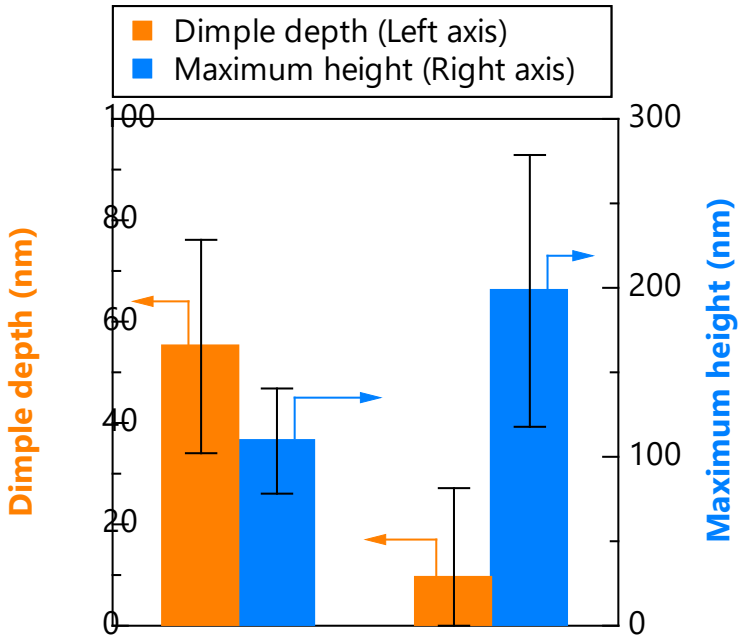
Dimple depth (Left axis)
Maximum height (Right axis)
Dimple depth (nm)
Maximum height (nm)
100
80
60
40
20
0
300
200
100
0
NPG
FG

(c)

FIG. 6

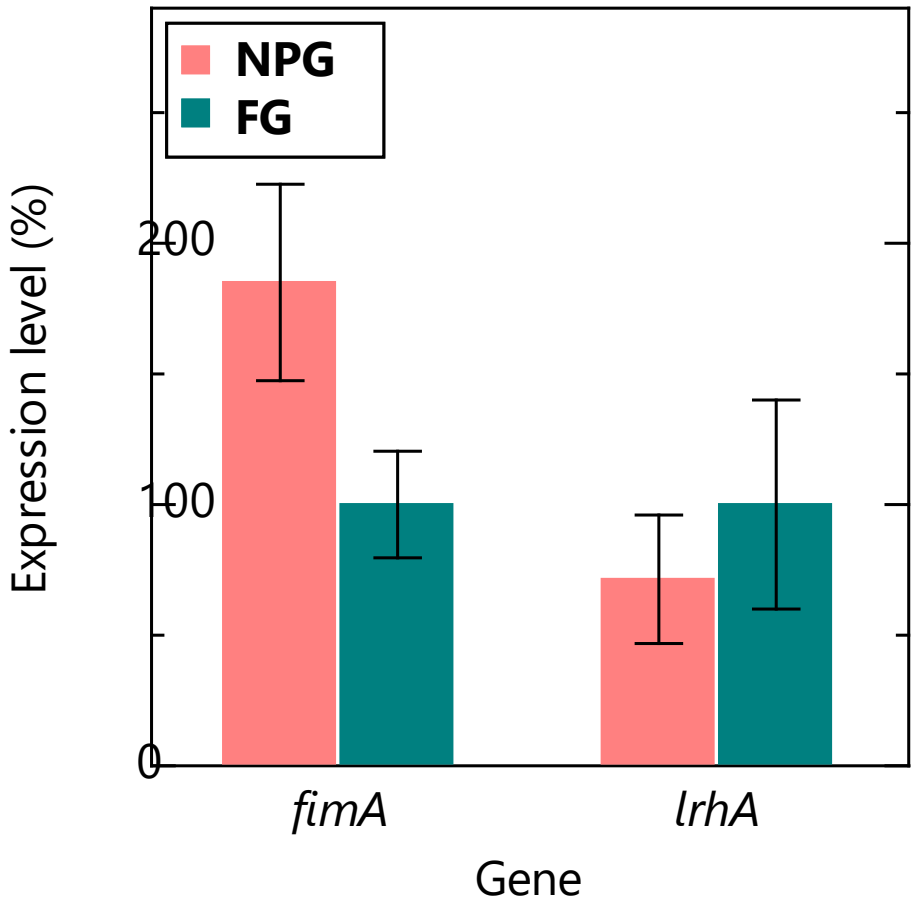

FIG. 6

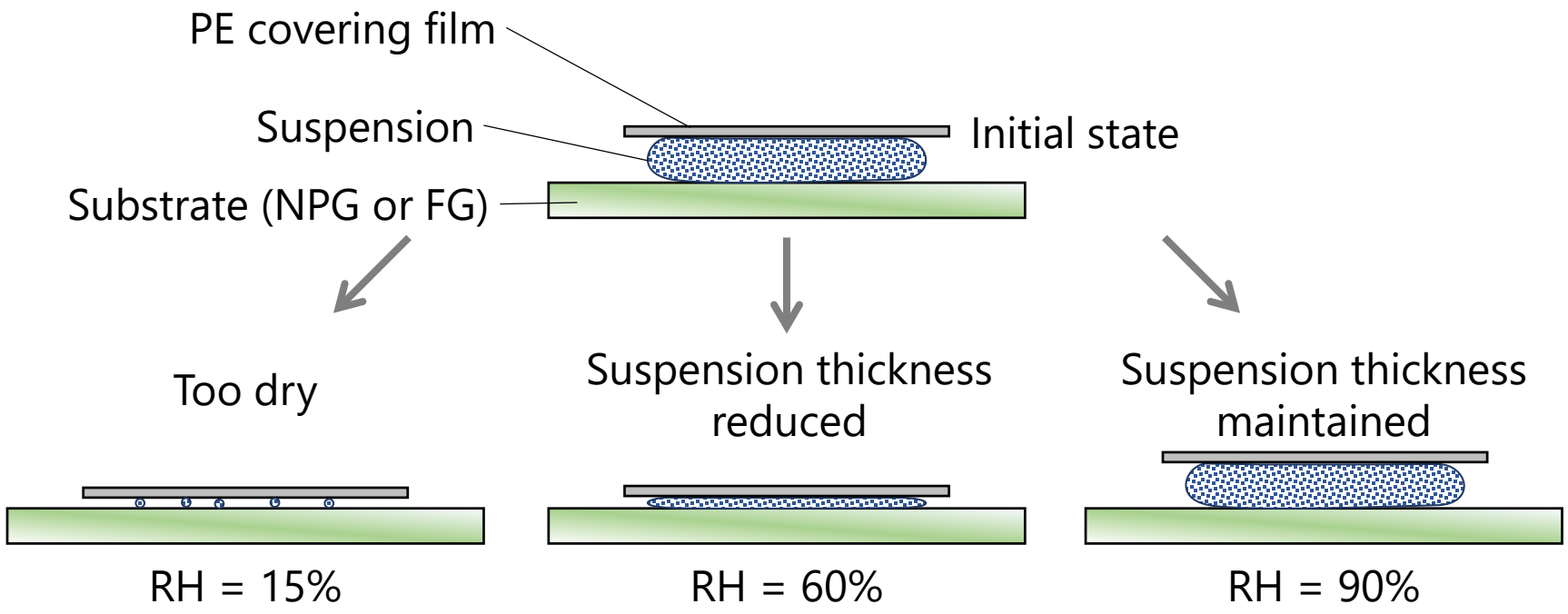
PE covering film
Suspension
Substrate (NPG or FG)
Initial state
Too dry
Suspension thickness reduced
Suspension thickness maintained
RH = 15%
RH = 60%
RH = 90%

FIG. 7

Supplementary Material for:

Antibacterial activity of nanoporous gold against *Escherichia coli* and *Staphylococcus epidermidis*

Masataka Hakamada*, Seiji Taniguchi†, Mamoru Mabuchi

Department of Energy Science and Technology, Graduate School of Energy Science, Kyoto University, Yoshidahonmachi, Sakyo, Kyoto 606-8501, Japan

* Corresponding author. E-mail: hakamada.masataka.3x@kyoto-u.ac.jp

† Present address: Sapporo Breweries Ltd., 2 Takasecho, Funahashi, Chiba 273-0014, Japan.

Energy-dispersive X-ray spectroscopy (EDXS) of nanoporous gold (NPG)

The results of EDXS of the synthesized NPG are shown in FIG. S1. The EDXS detected gold as well as other elements (oxygen, sodium, magnesium, silicon and potassium) in the glass substrate. No silver peaks were detected, which means that the residual Ag content in the NPG substrates was very small, being below the 1 at.% detection limit.

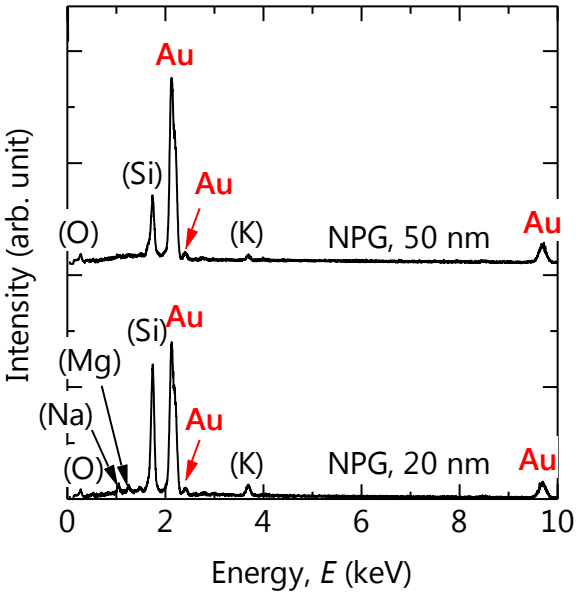

FIG. S1. EDXS results for NPG. The peaks of oxygen, sodium, magnesium, silicon and potassium come from glass substrates. (color online)

Scanning electron microscopy (SEM) image of flat gold (FG)

The SEM image of FG prepared by simple sputtering of gold on glass substrate is shown in FIG.S2. The polycrystalline and dense, but not porous, structure was observed.

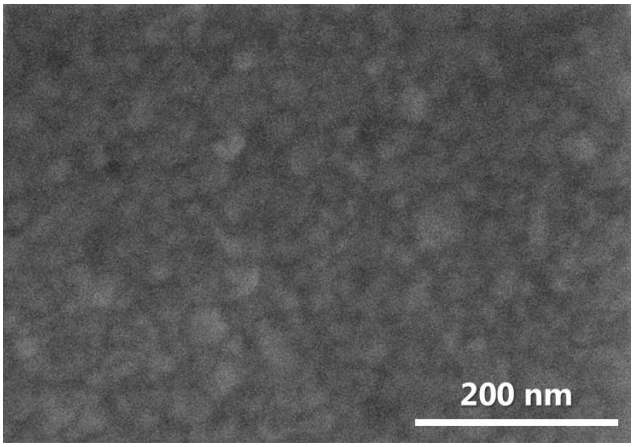

FIG. S2. SEM image for FG. Polycrystalline and dense, but not porous, structure was observed.

Time variation of viable bacterial counts (VBCs) on NPG and FG for *E. coli*

Figure S3 shows the variation in VBCs of *E. coli* on NPG and FG with incubation time, at a RH of 60%. The VBC on NPG was lower than that on FG at every incubation time. The VBCs on NPG incubated for 12–24 h were significantly lower than those on FG, at the corresponding incubation

times. The VBCs on NPG and FG were similar for incubation times of 0–12 h. Thus, antibacterial properties of NPG were evident after incubation for 12 h at a RH of 60%. This behavior is quite different from the antibacterial activity by metal ions, which typically begin decreasing the VBC immediately after commencing incubation.[1]

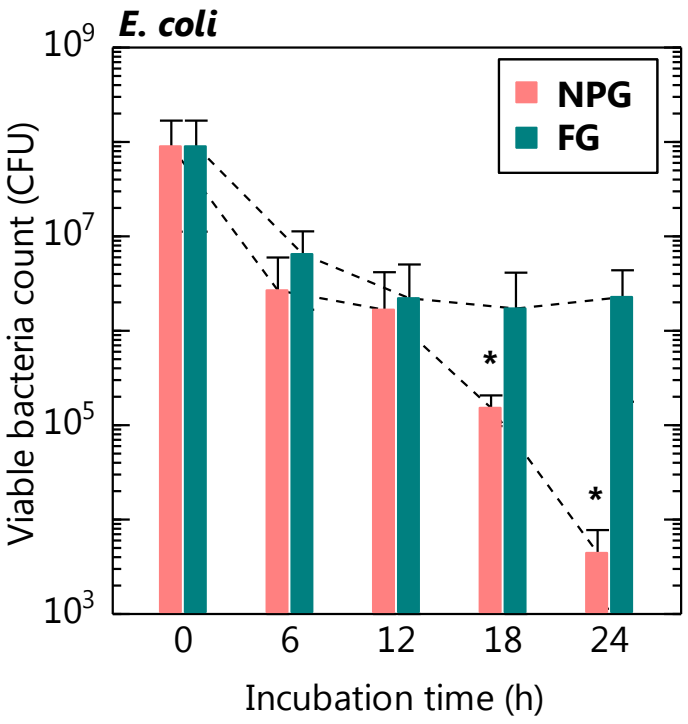

FIG. S3. Time variation of VBCs on NPG and FG for *E. coli*. * denotes significant difference between NPG and FG with $p < 0.01$. The VBC of *E. coli* on NPG significantly decreased after 12 h of incubation, while the VBC on FG did not. (color online)

Effect of metal ions on antimicrobial properties of NPG

The culturing solution was suspended on the nanoporous gold (NPG) substrate for 24 h, and the sample was then analyzed using inductively-coupled plasma atomic emission spectroscopy. The results are shown in FIG. S4. The concentrations of silver and gold in the culturing solutions were found to be < 0.05 ppm, which was the apparatus detection limit. It is well known that a concentration of at least approximately 1 ppm is necessary for realizing the antimicrobial properties of Ag ions.[1–4] Therefore, Ag ion dissolution from the NPG into the culturing solution was not responsible for the present antimicrobial properties of NPG.

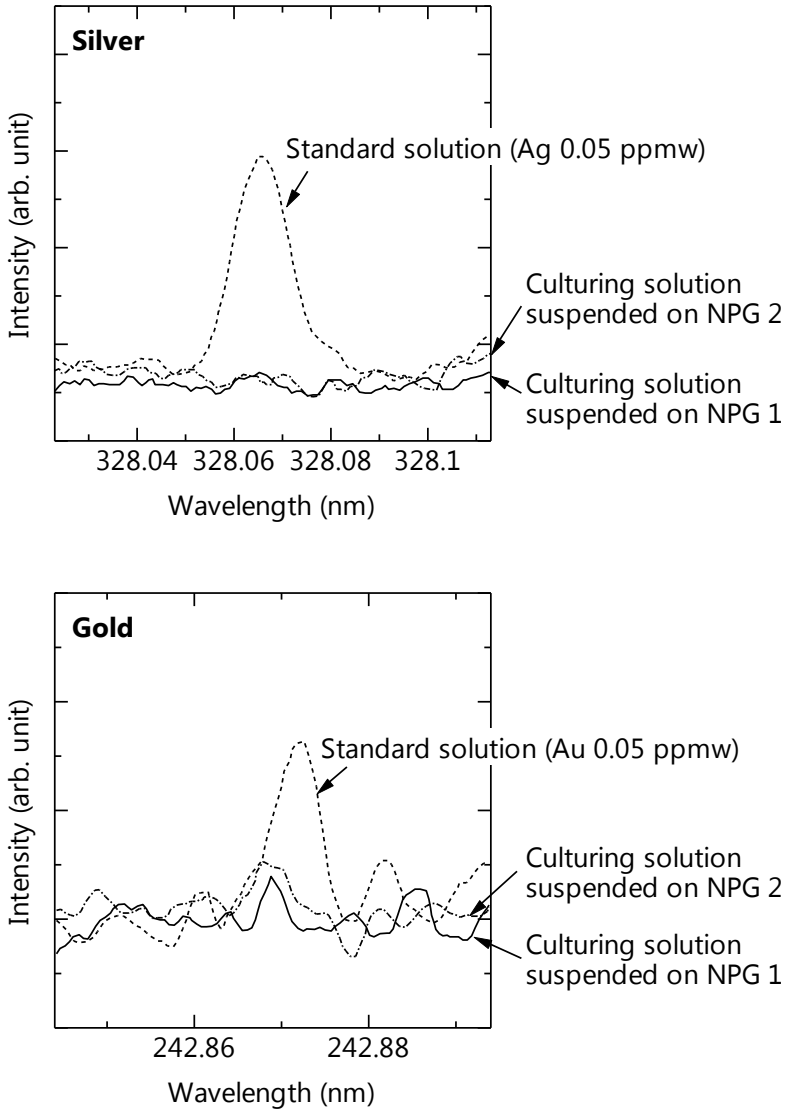

FIG. S4. The results of inductively-coupled plasma atomic emission spectroscopy analyses on culturing solution on NPG (pore size = 20 nm). No essential silver and gold dissolution was confirmed.

Effect of reactive oxygen species (ROS) on antimicrobial properties of NPG

We determined whether peroxides and reactive oxygen, which are known to be the main sources of the antimicrobial properties of copper, were responsible for the present antimicrobial properties of NPG.[5] We used the "Merckoquant peroxide test" to analyze the bacterial suspensions on the samples. First, the bacterial suspension used in the antimicrobial properties tests was incubated on NPG and FG for 12 h in humidity-controlled incubators at 298 K, under a relative humidity (RH) of 60%. Second, we immersed a test strip in the bacterial suspension for 1 s, to moisten the reaction area of the test paper. Third, we absorbed moisture on the test strip through the edge of the test strip for 15 s. Last, we compared the color of the reaction area with that of the color scale and read the corresponding values. The test strips immersed in the bacterial suspensions of both NPG and FG did not show any change in color, as shown in FIG. S5. Thus, the generation of ROS was excluded as a cause for the present antibacterial activity of NPG.

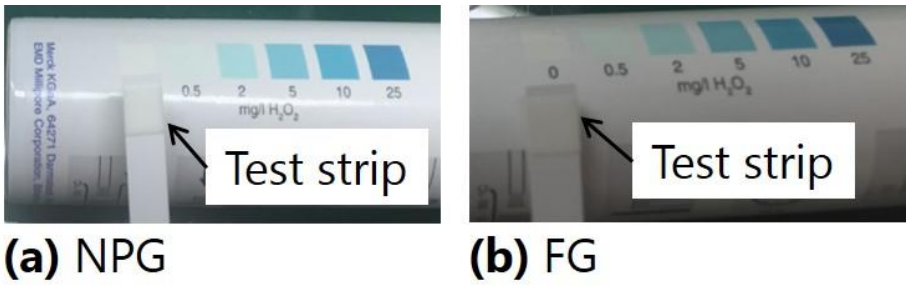

FIG. S5. The results of Merckoquant peroxide test on culturing solution on (a) NPG (pore size = 20 nm) and (b) FG. No essential ROS was confirmed. (color online)

References

1. Zhao, G. & Edward Stevens Jr, S. Multiple parameters for the comprehensive evaluation of the susceptibility of Escherichia coli to the silver ion. *BioMetals* **11,** 27–32 (1998).

2. Lok, C.-N., Ho, C.-M., Chen, R., He, Q.-Y., Yu, W.-Y., Sun, H., Tam, P. K.-H., Chiu, J.-F. & Che, C.-M. Proteomic analysis of the mode of antibacterial action of silver nanoparticles. *J. Proteome Res.* **5,** 916–924 (2006).

3. Randall, C. P., Oyama, L. B., Bostock, J. M., Chopra, I. & O'Neill, A. J. The silver cation (Ag^+): antistaphylococcal activity, mode of action and resistance studies. *J. Antimicrob. Chemother.* **68,** 131–138 (2013).

4. Miura, N. & Shinohara, Y. Cytotoxic effect and apoptosis induction by silver nanoparticles in HeLa cells. *Biochem. Biophys. Res. Commun.* **390,** 733–737 (2009).

5. Kumada, M., Akada, R., Kobuchi, K., Todoroki, Y. & Naotori, K. Clean anti-bacterial surface of copper. *J. JCBRA* **40,** 122–127 (2001) (in Japanese).